DETECTION OF SIMULATED ROOT PERFORATION IN THE VICINITY OF TITANIUM IMPLANT USING CBCT

Amr E. Elramah* , Raghdaa A. Mostafa** *and* Ashraf A. Abou-Khalaf***

ABSTRACT

Objectives: to evaluate the influence of the metal artifact reduction algorithm (MAR) on detecting root perforation adjacent to titanium implant using CBCT.

Materials and methods: This observational analytical *ex vivo* study was conducted on 56 human teeth. Two titanium implants were inserted in a dry human mandible at the site of the lower right and left first premolars. Then, decoronated single-rooted endodontically cleaned and shaped teeth were placed in the sockets adjacent to the implants. Of the 56 teeth, 28 were without perforation (control group), and 28 had simulated root perforations. CBCT scans were obtained without and with a metal artifact reduction filter and assessed by two dental radiologists and one general practitioner. Results were statistically analyzed in terms of accuracy, specificity, and sensitivity in addition to Kendall's coefficient of concordance and receiver operator characteristic (ROC) curve analysis.

Results: There was a significant difference between the results of acquisitions without and with the metal artifact reduction algorithm (MAR). Acquisitions without MAR had higher values; accuracy (91.1%) and sensitivity (92.9%). In contrast, acquisitions with MAR had lower values; accuracy (71.4%) and sensitivity (50%).

Conclusion: The metal artifact reduction algorithm hinders diagnosing lateral root perforation adjacent to titanium implants.

KEYWORDS: CBCT, root perforation, dental implants, MAR.

* Teaching Assistant in Oral and Maxillofacial Radiology Department, Faculty of Dentistry, Ain Shams University.
** Assistant Professor in Oral and Maxillofacial Radiology Department, Faculty of Dentistry, Ain Shams University.
*** Professor in Oral and Maxillofacial Radiology Department, Faculty of Dentistry, Ain Shams University.

INTRODUCTION

Root perforation is any pathological mechanical connection between the root canal system and the surrounding periodontium around the external tooth surface[1–3]. They can be caused by pathological processes such as internal or external root resorption, invasive dental caries, and aberrant canal morphology. These are called pathological perforations. In contrast, iatrogenic root perforations may occur during accidental errors in access cavity preparation, chemical-mechanical preparation, intracanal pin placement, post-space preparation, carelessness, or professional incompetence [3,4].

The complications of root perforation may result in an inflammatory reaction associated with periodontal tissue and alveolar bone destruction. It may cause granulomatous tissue development, epithelium proliferation, and, subsequently, periodontal pocket formation [5–7]. Because root perforation constitutes serious complications, it needs to be diagnosed early and appropriately treated [8,9].

Clinical and radiographical examinations are the basis of root perforation diagnosis. Several clinical findings can help in diagnosing root perforations. For example, persistent bleeding during coronal access or root canal preparation after removing the pulp tissue may indicate a perforation. A paper point soaked with blood may also suggest perforation. However, systemic conditions, medications, teeth with an open apex, internal resorption, and acute apical periodontitis may be associated with excessive bleeding and can be confused with root perforation[3,10–14]. Radiographically, a radiolucency associated with a connection between the root canal and the periodontal space is an important manifestation of perforation [15].

Periapical radiography is frequently indicated for endodontic diagnosis, treatment plan, and follow-up[11,12]. Despite its widespread use, it has limitations, which can lead to misdiagnosis and consequent incorrect treatment[16]. CBCT was introduced to overcome some of these limitations.

However, it has disadvantages, such as image quality degradation due to noise and contrast resolution. In addition, artifacts can occur because of high-density materials (HDMs), such as dental restorations and implants [5,17–21].

Dental implants are considered the best treatment option for tooth substitution in treating completely or partially edentulous individuals because of their masticatory functionality and predictable aesthetic outcomes[22,23]. Titanium is commonly used because of its chemical and physical properties and biocompatibility. These properties aid in osseointegration with the host bone so that acceptable anchorage and stability can be obtained for functional dental restorations[24–26].

As implants marketed nowadays are composed of high-density elements, generating artifacts in their CBCT images is unavoidable. The effect of these artifacts around the implant can hinder the accurate evaluation of the implants themselves or the adjacent structures. Implants present in the scanned region, in examinations done for other needs, can hinder image quality, such as using CBCT to detect proximal caries[27], vertical root fracture[28], or furcal root perforation in teeth adjacent to titanium implants[29].

Nowadays, almost all CBCT scanners have metal artifact reduction (MAR) tools in different ways. The MAR algorithms used in image processing aim to decrease or, if possible, eliminate artifacts, thus increasing the image quality [30–33].

Some studies have attempted to study the influence of applying a post-processing metal artifact reduction (MAR) algorithm in detecting vertical root fracture (VRF) in teeth adjacent to implants [28,34,35]. In addition, some attempted to study the effect of MAR in detecting root perforation and VRF adjacent to different intracanal sealer materials [29,36]. Although some studies showed a negative impact of MAR application on diagnostic accuracy[35,37], other studies showed an objective improvement in image quality using MAR [31,33,38–41]. However, in many

cases, even the improvement in image quality does not reflect a better clinical diagnosis by applying MAR [42].

Oliveira et al. [35] reported that MAR negatively influenced VRF detection using CBCT. Similarly, Sheikhi et al.[43] concluded that the MAR algorithm does not increase the CBCT detection accuracy of fenestration and dehiscence around the dental implant. Moreover, Kamburoğlu et al.[44] showed no difference between CBCT images obtained with and without MAR modes in detecting peri-implant bony defects. Furthermore, De-Azevedo et al. [45] observed that the MAR algorithm did not improve the diagnosis of peri-implant fenestrations and dehiscences. In contrast, Kamburoğlu et al. [29] reported that MAR performed well in detecting furcal perforation in the presence of different sealer materials and metallic posts. Moreover, Koc et al. [46] showed MAR has a good influence in detecting strip root perforation with intracanal sealer material.

The diagnostic benefit of MAR is questionable. Furthermore, in the dentomaxillofacial radiology field, the MAR is still considered a black box because the manufacturers do not provide enough information on how the algorithms act on the image quality[30,32]. However, to our knowledge, there is limited information about the influence of the MAR tool on CBCT root perforation detection adjacent to titanium implants. Thus, this study aimed to investigate the influence of the MAR tool on the diagnosis of root perforations in a tooth adjacent to a titanium implant in CBCT images.

MATERIAL AND METHODS

Study Design and Sample Selection

This ex vivo diagnostic accuracy study was planned and performed according to STARD guidelines[47]. Sample size calculation was done according to the study's findings by **Fontenele, and Gomes** [34], considered the closest study to the current one, by adopting an alpha of 0.05. A beta of 0.1, i.e., power = 90% of the predicted sample size

(n), was found to be 40 teeth, but we increased this to 56 teeth to increase the reliability of the results and decrease margins of error.

Mandible selection

One dry human mandible (anonymized age and gender) was borrowed from the Department of Anatomy, Faculty of Medicine, Ain Shams University. Dental implant osteotomies were made in the right and left mandibular first premolar region using sequential drilling; Pilot drill 2.2 mm / Twist drill 2.8, 3.2, 3.8, 4.2 mm. Then, two identical implants with the size of 4.2 X 13 mm (MPI plus implant, Vitronex, Italy) were inserted in their corresponding osteotomies. Next, the whole mandible was covered by three layers of softened pink wax (Cavex, Haarlem, Germany) to simulate soft tissue density during image acquisition (**Figure 1**).

Fig. (1) Dry human mandible covered with softened pink wax with two titanium implants in place.

Preparation of teeth with simulated root perforation

The sample consisted of 56 human single-rooted mandibular teeth (canines and second premolars) extracted for periodontal or orthodontic reasons. These teeth were collected from a pooled bio-bank, so the local ethical committee categorized the samples as "irreversibly anonymized," No previous approval was necessary.

Teeth with previous endodontic treatment, external or internal root resorption, root caries, cracks, fractures, unmatured apices, and calcified root canals were excluded. Teeth were cleaned of calculus and debris by scaling. Then, they were disinfected for 20 minutes in a 2% sodium hypochlorite solution and stored in distilled water. Next, teeth were divided into four equal groups (14 right mandibular canines, 14 mandibular right second premolar, 14 left mandibular canines, and 14 mandibular left second premolar). Each group was placed in a separate plastic bag. Different colors were assigned for each group; blue for lower right canines, white for lower right second premolars, red for lower left canines, and black for lower left second premolars.

The main researcher carried out access cavities, cleaning and shaping each tooth using the gold Pro-Taper rotary system (Dentsply Maillefer, Ballaigues, Switzerland). The canal patency was obtained by #10 K-files (Mani Inc, Utsunomiya, Tochigi, Japan). One mL of 2.5% sodium hypochlorite as the irrigating solution was used between instruments. Next, teeth were decoronated at the cementoenamel junction (CEJ) level to avoid bias related to the recognition of coronary features during the evaluations. These steps were repeated for each tooth within the four groups previously mentioned **(Figure 2).**

Within each group, teeth were divided into two equal subgroups to perform root perforation (7 control and seven perforated). Perforations were done using size #15 C+ Endodontic stainless-steel file (Dentsply Maillefer, Ballaigues, Switzerland) mounted on engine-driven low-speed handpiece

10:1 reduction contra angle (model number: CX235C5 Coxo Inc, Foshanchen, Guangdong, China). The rotating file was inserted inside the canal at approximately 45 degrees to the horizontal plane. This creates perforation on the proximal surface with a 0.15mm diameter at approximately 5 mm from the CEJ **(Figure 3).** Canines had simulated perforations in their distal surfaces, while second premolars had simulated perforations in their mesial surfaces. The perforated teeth were then put back into their corresponding bags.

Fig. (2) Decoronated teeth; a color was assigned to each group: blue for right canines, white for right second premolar, red for left canines, and black for left second premolars.
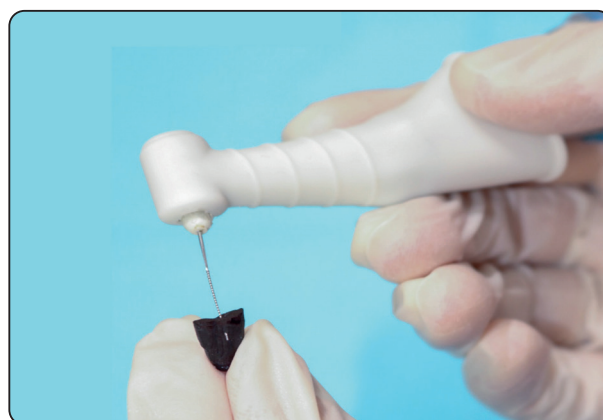

Fig. (3) Perforation was done by inserting the rotating file inside the canal.

For randomization, a general dentist not participating in the study chose one random tooth from each of the four groups and examined whether it was perforated or not (control). Those four selected teeth were placed in a separate bag and given a sequential number from 1 to 14. This process was repeated for all the teeth in each group (**Figure. 4**). A chart was created to document the content of each of the 14 bags unknown to the observers.

Image acquisition, Observation, and Scoring:

Before CBCT acquisition, teeth in bag number 1 were mounted in their corresponding sockets in the mandible. Standardized CBCT scans for the mandible were obtained using the Planmeca Promax-s scanner (Planmeca, Helsinki, Finland). The scanning parameters were a 5 X 5 cm FOV, 90 KVP, 14 mA, and 0.1 mm. The metal artifact reduction (MAR) filter was not selected. The mandible was stabilized using a strengthened paper box mounted on the supporting plate of the machine. The mandible midline was adjusted with the anterior vertical laser light, while the posterior vertical laser light was placed just to the mandibular canines to centralize the mandible in the FOV in the anterior-posterior direction. The horizontal laser light was adjusted to be parallel to the occlusal plane of the teeth. The scan was given a number identical to the corresponding bag (**Figure 5**).

After scan acquisition, a post-acquisition MAR filter was applied. This resulted in two reconstructions for each scan. These steps were repeated for all 14 bags. Within each scan, there were two reconstructions (one without the MAR filter and one with the post-acquisition MAR filter). Hence, 28 reconstructed volumes were obtained (14 scans × 2). Next, images were exported as single-frame multiple DICOM files using Planmeca Romexis® software (Planmeca, Helsinki, Finland).
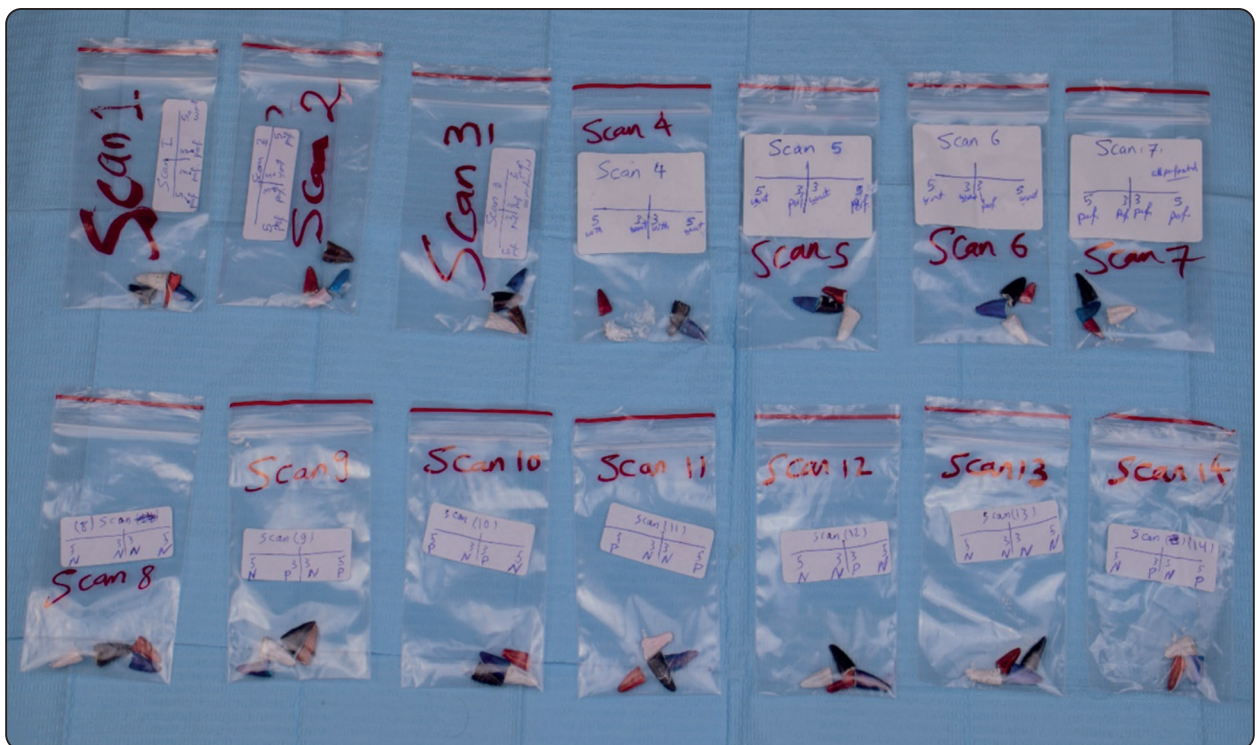

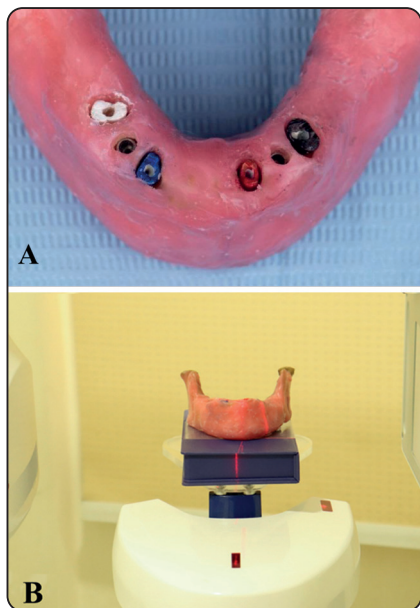Fig. (4) Grouping and randomization of teeth.

Fig. (5) A: Before image acquisition, implants and teeth in their places B: Positioning the mandible for CBCT scanning.

For evaluation, images were imported on Ondemand3ddental software (Cybermed, Seoul, Republic of Korea). For randomization during importing, each volume was given a random number (from 1 to 28) known only by the general dentist responsible for randomization and scanning so that all the observers were blinded.

A total of 28 datasets of CBCT images were examined by three examiners: Two radiologists (one with nine years of experience and one with eight years' experience) and one general practitioner. Before the initial evaluation, a calibration session was conducted using images from each radiographic protocol to standardize the radiological assessment of perforation detection. The observers were entitled to manipulate the whole volume freely and use software enhancement tools to detect the perforations. All observers were informed to use a three-grade scoring system to describe their observations: Score 1: Perforation is definitely present. Score 2: uncertain/unable to tell. Score 3: Perforation is definitely not present.

After the first session, each observer independently examined the 28 reconstructed volumes and recorded their scores in an Excel sheet. After one month, each observer reevaluated the observations independently to determine the intra-observer agreement.

Statistical analysis

Inter and intra-rater reliability were analyzed using Kendall's coefficient of concordance. Sensitivity, specificity, and area under the ROC curve (AUC) values were calculated to determine the diagnostic ability of CBCT to detect perforation in teeth adjacent to titanium implants and were compared using the z-test. The significance level was set at $p \leq 0.05$ for all tests. Statistical analysis was performed with R statistical analysis software version 4.1.3 for Windows [48].

RESULTS

The intra-observer reliability ranged from 0.940 to 0.992, indicating strong agreement between both observations for all observers (table 1). The inter-observer reliability was 0.81, indicating a strong agreement between observers (table 2).

TABLE (1) Intra-observer reliability for different groups.

Observer	Kendall's W	χ^2	p-value
1st observer	0.980	217.48	<0.001*
2nd observer	0.992	220.24	<0.001*
3rd observer	0.940	208.66	<0.001*

*; significant (p ≤ 0.05) ns; non-significant (p>0.05)

TABLE (2) Inter-observer reliability for different groups.

Kendall's W	χ^2	p-value
0.817	546.62	<0.001*

*; significant (p ≤ 0.05) ns; non-significant (p>0.05)

The area under the ROC curve (AUC values) for detection of root perforation was calculated without MAR and with MAR scans (Table 3). AUC values were between 0.911 and 0.925 for detecting perforation without MAR and between 0.714 and 0.777 for detecting perforation with MAR. According to AUC values, the application of the MAR tool decreased the diagnostic accuracy for the detection of root perforation.

Sensitivity, specificity, and accuracy for both MAR modes were calculated independently for detecting root perforation (table 4). Accuracy and sensitivity values without MAR were higher than with MAR, while specificity values were almost the same in both modes.

TABLE (3) AUC for CBCT-based detection of root perforation without and with MAR.

	AUC		AUC 95% CI		SE		Z-value	P-value
	Without MAR	With MAR	Without MAR	With MAR	Without MAR	With MAR		
1st observer	0.925	0.731	0.855:0.996	0.625:0.837	0.04	0.07	3.09	0.002*
2nd observer	0.911	0.714	0.835:0.987	0.596:0.831	0.04	0.07	3.8	<0.001*
3rd observer	0.924	0.777	0.853:0.995	0.665:0.888	0.04	0.06	2.28	0.023*

AUC, area under the curve; CI, confidence interval; SE, standard error *; significant (p ≤ 0.05) ns; non-significant (p>0.05)

TABLE (4) Percentage sensitivity and specificity of CBCT images without and with MAR in detecting root perforation.

	1st observer		2nd observer		3rd observer	
	Without MAR	With MAR	Without MAR	With MAR	Without MAR	With MAR
Sensitivity	92.9%	50%	89.3%	53.6%	92.9%	57.1%
Specificity	89.3%	92.9%	92.9%	89.3%	89.3%	92.9%
False positive rate	10.7%	7.1%	7.1%	10.7%	10.7%	7.1%
Positive predictive value	89.7%	87.5%	92.6%	83.3%	89.7%	88.8%
Negative predictive value	92.6%	65%	89.7%	65.8%	92.6%	68.4%

DISCUSSION

Proper diagnosis of root perforations represents a real concern for dental practitioners to assess tooth restorability and prognosis [49]. CBCT is a powerful diagnostic tool for detecting root perforation. Still, its perforation detection accuracy is hindered by beam hardening artifacts generated by HDMs like titanium implants adjacent to these perforations [50,51].

A dry human mandible was used as an ex-vivo phantom, similar to a study by **Gaalaas et al.** [52]. The teeth were adapted with their roots into the empty sockets to simulate the real dental arch as much as possible. The mandible was covered with three layers of softened pink wax buccally and lingually to simulate the attenuation properties of the soft tissues during CBCT scanning. Similarly, **Baltacioĝlu et al.** [53] covered the dry skull and mandible with 2-cm red wax as a soft-tissue equivalent material during CBCT scanning to detect recurrent caries.

Titanium implants were used because titanium is one of the most commonly used dental implant materials [54]. In our daily practice, there is a high probability of seeing patients with one or more titanium implants in their oral cavities. In addition, the beam hardening artifacts produced by these implants in CBCT images need more investigations according to the recommendations of **Vasconcelos et al**. [51] and **Gaêta et al.** [55].

Endodontic treatment was performed using Gold Protaper rotary files to ensure standardized canal preparation of all teeth. The prepared canal morphology was the same size and shape for all teeth to prevent root canal recognition during the evaluation. Like Fontenele, and Gomes[34], teeth were decoronated at the CEJ level to avoid bias related to the recognition of coronary features or memorization of the tooth during the evaluations.

Based on **Senthilkumar et al.** [56], root perforation at the level of crestal bone has the worst prognosis among different perforation types; therefore, in the current study, 0.15 mm perforation was done at approximately 5 mm apical to the CEJ from internal to the external root surface. This technique was adopted to simulate the clinical situation as close as possible.

Planmeca Promax-s scanner (Planmeca, Helsinki, Finland) was utilized as it allows the application of MAR before or after image acquisition. The problem with the pre-acquisition MAR filter is that it cannot be removed after the acquisition. The practitioner must capture two scans, one with and one without MAR, to compare the resulting images. In clinical situations, this necessitates patients' exposure twice, which is ethically unacceptable. Therefore, post-acquisition MAR was used in this study as it generates two reconstructions from the same scan.

Fontenele et al. [41] found that both modes of MAR activations (pre and post-acquisition) effectively decreased the magnitude of CBCT artifacts generated by zirconium implants using OP300 Maxio CBCT unit (Instrumentarium Dental, Tuusula, Finland). Similarly, **Shahmirzadi et al.** [57] showed no difference between pre-and post-acquisition MAR in decreasing beam hardening artifacts using the Planmeca CBCT machine (ProMax® 3D Max; Planmeca, Helsinki, Finland).

Vasconcelos et al. [57] and **Freitas et al.** [38] reported that increasing KVp would decrease the amount of HDMs artifacts in CBCT images. Moreover, **Gaêta-Araujo et al.** [54] reported that increasing the tube current would have the same effect. In the current study, 90 KVp and 14 mA, the highest kilovoltage and tube current available in the machine, were used to ensure the best exposure settings were utilized and that the only factor that might interfere with the radiographic diagnosis of simulated perforation would be the artifacts produced by adjacent Ti implants.

This study used a 0.1 mm voxel size, similar to **Orhan et al.** [58] and **Koç et al.** [59], who concluded

that 0.1 mm is preferred to get the best spatial resolution for detecting endodontic complications. This ensures that the only limitation that could stand against perforation detection was the beam hardening artifact taking observer experience and ability to detect perforations into consideration.

The results of the current study showed strong agreement in both intra- and interobserver reliability. Likewise, **Kamburoğlu et al.** [29] reported excellent intraobserver reliability and strong interobserver reliability in CBCT furcal perforation detection in teeth with different intracanal sealer materials and posts. Similarly, **Koc et al.** [46] showed moderate to excellent agreement for inter- and intraobserver reliability in detecting different endodontic complications using different CBCT units and different MAR modes. The authors explained that this agreement might be due to the well-trained dentists acting as observers and the ex vivo setup that caused no motion and few beam hardening artifacts. For these reasons, clinicians should be cautious when extrapolating the results of a laboratory study on CBCT compared to a clinical situation because, in real-life conditions, each patient's body interacts differently with the X-ray beam [40].

In addition, **Fontenele and Gomes** [34] found reasonable to excellent agreement for both intra- and interobserver reliability in VRF detection in teeth adjacent to zirconium implants with different tube currents and MAR modes. Moreover, **Freitas et al.** [28] showed intra- and interobserver agreements ranged from substantial to excellent and fair to substantial in detecting VRF near zirconium implants using different kVp settings, with and without MAR applied.

Regarding the comparison between the accuracy of CBCT in detecting simulated root perforation in teeth adjacent to titanium implants in images without and with MAR, the sensitivity of CBCT in images without MAR was higher than in images with MAR. The specificity of both modes was almost the same for all observers. In addition, the accuracy in the images without MAR was higher than with MAR, as confirmed by AUC and accuracy test, and the difference was statistically significant. The results of the current study reflected that the Promax MAR algorithm did not reduce the artifacts accurately. Therefore, it is not leading to a more accurate diagnosis of root perforation.

In contrast, **Kamburoğlu et al.** [29] reported that AUC values were high in both images without and with MAR applied in detecting furcal perforation in the presence of different sealer materials and metallic posts. Moreover, **Koc et al.** [46] showed high AUC values in both modes without and with MAR in detecting strip root perforation with intracanal sealer material. The perforation size and technique could explain the difference between our results and theirs. **Kamburoğlu et al.** [29] made a perforation size of 0.97 mm using round bur, while **Koc et al.** [46] made a perforation size of 0.9 mm using Gates Glidden. In this study, 0.15 mm size perforations were done using a rotating size 15 C-plus file. The Promax MAR tool inaccurately corrected the 0.15 mm perforation, considering it an artifact, and subsequently removed it. In comparison, the 0.9- and 0.97-mm perforations were larger, so MAR correction did not remove them completely, so their detection was unaffected.

In agreement with our results, **Oliveira et al.** [35] reported a decrease in AUC and sensitivity with MAR in detecting VRF in teeth with metallic posts. In contrast, they reported reduced specificity values. This could be due to the difference in scanners, the MAR tool, and the high-density material used.

CONCLUSION

Within the limitations of this study, we can conclude that the MAR algorithm compromises perforation detection in teeth adjacent to the titanium implants.

List of Abbreviations

AR	Artifact Reduction
CBCT	Cone Beam Computed Tomography
CEJ	Cementoenamel junction
DICOM	Digital Imaging and Communications in Medicine
FOV	Field of view
HDMs	High-Density Materials
kVp	Kilovoltage peak
mA	Milliampere
MAR	Metal Artifact Reduction
MPR	Multiplanar Reconstruction
VRF	Vertical root fracture
ROC curve	Receiver operating characteristic curve.
AUC	The area under the curve. **Declaratio**

Competing interests

The authors declare they have no conflict of interest.

Funding

No funding is subjected to the research reported in this manuscript.

Ethics approval and consent to participate.

Ethical approval was obtained from the ethical committee of the faculty of dentistry at Ain Shams University (code: FDASU_RecEMI22011). All methods were carried out in accordance with relevant guidelines and regulations. All experimental protocols were approved by the local ethics committee of the faculty of dentistry at Ain Shams University. The teeth were collected from a pooled bio-bank, so the local ethical committee categorized the samples as "irreversibly anonymized," No previous approval was necessary. Informed consent was waived by the ethics committee of the faculty of dentistry at Ain Shams University (code: FDASU_RecEMI22011).

Availability of data and materials

All data included in this study are available from the corresponding author upon request.

REFERENCES

1. American Association of Endodontists. Glossary of Endodontic Terms 2016. Gloss Endod Terms [Internet]. 2015;9:43. Available from: http://www.nxtbook.com/nxtbooks/aae/endodonticglossary2016/#/0

2. American Association of Endodontists. Glossary of Endodontic Terms. 2012;8th.

3. Tsesis I, Fuss Z. Diagnosis and treatment of accidental root perforations. Endod Top [Internet]. 2006;13(1):95–107. Available from: https://onlinelibrary.wiley.com/doi/10.1111/j.1601-1546.2006.00213.x

4. Estrela C, Decurcio DA, Rossi-Fedele G, et al. Root perforations: a review of diagnosis, prognosis, and materials. Braz Oral Res 2018;32:133–46.

5. Estrela C, Decurcio D de A, Rossi-Fedele G, Silva JA, Guedes OA, Borges ÁH. Root perforations: A review of diagnosis, prognosis, and materials. Braz Oral Res. 2018;32:133–46.

6. Touré B, Faye B, Kane AW, Lo CM, Niang B, Boucher Y. Analysis of reasons for extraction of endodontically treated teeth: A prospective study. J Endod. 2011;37(11):1512–5.

7. Holland R, Arlindootobonifilho J, Desouza V, Juvenalnery M, Felicioestradabernabe P, Dezanjunior E. Mineral Trioxide Aggregate Repair of Lateral Root Perforations. J Endod [Internet]. 2001 Apr;27(4):281–4. Available from: http://linkinghub.elsevier.com/retrieve/pii/S0099239905607492

8. Farzaneh M, Abitbol S, Friedman S. Treatment outcome in endodontics: The Toronto study. Phases I and II: Orthograde retreatment. J Endod. 2004 Sep 1;30(9):627–33.

9. Clauder T, Shin S-J. Repair of perforations with MTA: clinical applications and mechanisms of action. Endod Top [Internet]. 2006 Nov;15(1):32–55. Available from: https://onlinelibrary.wiley.com/doi/10.1111/j.1601-1546.2009.00242.x

10. Fuss Z, Trope M. Root perforations: Classification and treatment choices based on prognostic factors. Endod Dent Traumatol [Internet]. 1996 Dec;12(6):255–64. Available from: https://onlinelibrary.wiley.com/doi/10.1111/j.1600-9657.1996.tb00524.x

11. Grossman LI, Shepard LI, Pearson LA. Roentgenologic and clinical evaluation of endodontically treated teeth. Oral Surgery, Oral Med Oral Pathol [Internet]. 1964 Mar;17(3):368–74. Available from: https://linkinghub.elsevier.com/retrieve/pii/0030422064905109

12. Seltzer S, Bender IB, Smith J, Freedman I, Nazimov H. Endodontic failures-An analysis based on clinical, roentgenographic, and histologic findings. Part I. Oral Surgery, Oral Med Oral Pathol [Internet]. 1967 Apr;23(4):500–16. Available from: https://linkinghub.elsevier.com/retrieve/pii/0030422067905464

13. Estrela C, Holland R, Estrela CR de A, Alencar AHG, Sousa-Neto MD, Pécora JD. Characterization of Successful Root Canal Treatment. Braz Dent J [Internet]. 2014 Jan;25(1):3–11. Available from: http://www.scielo.br/scielo.php?script=sci_arttext&pid=S0103-64402014000100003&lng=en&tlng=en

14. Silva JA, Alencar AHG de, Rocha SS da, Lopes LG, Estrela C. Three-dimensional image contribution for evaluation of operative procedural errors in endodontic therapy and dental implants. Braz Dent J [Internet]. 2012 Apr;23(2):127–34. Available from: http://www.scielo.br/scielo.php?script=sci_arttext&pid=S0103-64402012000200007&lng=en&tlng=en

15. Takeshita WM, Chicarelli M, Iwaki LCV. Comparison of diagnostic accuracy of root perforation, external resorption, and fractures using cone-beam computed tomography, panoramic radiography, and conventional & digital periapical radiography. Indian J Dent Res. 2015;26(6):619–26.

16. Use of cone-beam computed tomography in endodontics Joint Position Statement of the American Association of Endodontists and the American Academy of Oral and Maxillofacial Radiology. Oral Surgery, Oral Med Oral Pathol Oral Radiol Endodontology [Internet]. 2011 Feb;111(2):234–7. Available from: https://linkinghub.elsevier.com/retrieve/pii/S1079210410008887

17. Schulze R, Heil U, Groß D, Bruellmann DD, Dranischnikow E, Schwanecke U, et al. Artefacts in CBCT: A review. Dentomaxillofacial Radiol. 2011;40(5):265–73.

18. Draenert F, Coppenrath E, Herzog P, Müller S, Mueller-Lisse U. Beam hardening artefacts occur in dental implant scans with the NewTom ® cone beam C.T. but not with the dental 4-row multidetector C.T. Dentomaxillofacial Radiol [Internet]. 2007 May;36(4):198–203. Available from: http://www.birpublications.org/doi/10.1259/dmfr/32579161

19. Pauwels R, Araki K, Siewerdsen JH, Thongvigitmanee SS. Technical aspects of dental CBCT: state of the art. Dentomaxillofacial Radiol [Internet]. 2015 Jan;44(1):20140224. Available from: http://www.birpublications.org/doi/10.1259/dmfr.20140224

20. Katsumata A, Hirukawa A, Noujeim M, Okumura S, Naitoh M, Fujishita M, et al. Image artifact in dental cone-beam C.T. Oral Surgery, Oral Med Oral Pathol Oral Radiol Endodontology [Internet]. 2006 May;101(5):652–7. Available from: https://linkinghub.elsevier.com/retrieve/pii/S1079210405006189

21. Azevedo B, Lee R, Shintaku W, Noujeim M, Nummikoski P. Influence of the Beam Hardness on Artifacts in Cone-Beam CT. Oral Surgery, Oral Med Oral Pathol Oral Radiol Endodontology [Internet]. 2008 Apr;105(4):e48. Available from: https://linkinghub.elsevier.com/retrieve/pii/S1079210408000747

22. Cinquini C, Marchio V, Di Donna E, Alfonsi F, Derchi G, Nisi M, et al. Histologic Evaluation of Soft Tissues around Dental Implant Abutments: A Narrative Review. Materials (Basel) [Internet]. 2022 May 27;15(11):3811. Available from: https://www.mdpi.com/1996-1944/15/11/3811

23. Buser D, Sennerby L, De Bruyn H. Modern implant dentistry based on osseointegration: 50 years of progress, current trends, and open questions. Periodontol 2000 [Internet]. 2017 Feb;73(1):7–21. Available from: https://onlinelibrary.wiley.com/doi/10.1111/prd.12185

24. Bruschi M, Steinmüller-Nethl D, Goriwoda W, Rasse M. Composition and Modifications of Dental Implant Surfaces. J Oral Implant [Internet]. 2015 Jan 12;2015:1–14. Available from: https://www.hindawi.com/journals/joi/2015/527426/

25. Demirturk Kocasarac H, Ustaoglu G, Bayrak S, Katkar R, Geha H, Deahl ST, et al. Evaluation of artifacts generated by titanium, zirconium, and titanium–zirconium alloy dental implants on MRI, CT, and CBCT images: A phantom study. Oral Surg Oral Med Oral Pathol Oral Radiol [Internet]. 2019;127(6):535–44. Available from: https://doi.org/10.1016/j.oooo.2019.01.074

26. Guo T, Gulati K, Arora H, Han P, Fournier B, Ivanovski S. Race to invade: Understanding soft tissue integration at the transmucosal region of titanium dental implants. Dent Mater. 2021;37(5):816–31.

27. Abu El-Ela WH, Farid MM, Abou El-Fotouh M. The impact of different dental restorations on detection of proximal caries by cone beam computed tomography. Clin Oral Investig. 2022;26(3):2413–20.

28. Freitas DQ, Vasconcelos TV, Noujeim M. Diagnosis of vertical root fracture in teeth close and distant to implant: an in vitro study to assess the influence of artifacts

produced in cone beam computed tomography. Clin Oral Investig. 2019;23(3):1263–70.

29. Kamburoğlu K, Yilmaz F, Yeta EN, Özen D. Assessment of furcal perforations in the vicinity of different root canal sealers using a cone beam computed tomography system with and without the application of artifact reduction mode: An ex vivo investigation on extracted human teeth. Oral Surg Oral Med Oral Pathol Oral Radiol. 2016;121(6):657–65.

30. Gjesteby L, De Man B, Jin Y, Paganetti H, Verburg J, Giantsoudi D, et al. Metal Artifact Reduction in CT: Where Are We After Four Decades? IEEE Access [Internet]. 2016;4:5826–49. Available from: http://ieeexplore.ieee.org/document/7565564/

31. Queiroz PM, Santaella GM, da Paz TDJ, Freitas DQ. Evaluation of a metal artefact reduction tool on different positions of a metal object in the FOV. Dentomaxillofacial Radiol [Internet]. 2017 Mar;46(3):20160366. Available from: http://www.birpublications.org/doi/10.1259/dmfr.20160366

32. Katsura M, Sato J, Akahane M, Kunimatsu A, Abe O. Current and Novel Techniques for Metal Artifact Reduction at CT: Practical Guide for Radiologists. RadioGraphics [Internet]. 2018 Mar;38(2):450–61. Available from: http://pubs.rsna.org/doi/10.1148/rg.2018170102

33. Nascimento EHL, Fontenele RC, Santaella GM, Freitas DQ. Difference in the artefacts production and the performance of the metal artefact reduction (MAR) tool between the buccal and lingual cortical plates adjacent to zirconium dental implant. Dentomaxillofacial Radiol [Internet]. 2019 Dec;48(8):20190058. Available from: https://www.birpublications.org/doi/10.1259/dmfr.20190058

34. Fontenele RC, Gomes AF. Do the tube current and metal artifact reduction influence the diagnosis of vertical root fracture in a tooth positioned in the vicinity of a zirconium implant ? A CBCT study. 2020;

35. Oliveira MR, Sousa TO, Caetano AF, de Paiva RR, Neto JV, Yamamoto Silva FP, et al. Influence of CBCT metal artifact reduction on vertical radicular fracture detection. Imaging Sci Dent [Internet]. 2021 Mar;51(1):1–8. Available from: https://doi.org/10.5624/isd.20200191

36. Chang E, Lam E, Shah P, Azarpazhooh A. Cone-beam Computed Tomography for Detecting Vertical Root Fractures in Endodontically Treated Teeth: A Systematic Review. J Endod [Internet]. 2016;42(2):177–85. Available from: http://dx.doi.org/10.1016/j.joen.2015.10.005

37. Bechara B, McMahan CA, Moore WS, Noujeim M, Teixeira FB, Geha H. Cone beam C.T. scans with and without artefact reduction in root fracture detection of endodontically treated teeth. Dentomaxillofacial Radiol. 2013;42(5).

38. Freitas DQ, Fontenele RC, Nascimento EHL, Vasconcelos TV, Noujeim M. Influence of acquisition parameters on the magnitude of cone beam computed tomography artifacts. Dentomaxillofacial Radiol. 2018;47(8).

39. Fontenele RC, Nascimento EHL, Vasconcelos T V., Noujeim M, Freitas DQ. Magnitude of cone beam C.T. image artifacts related to zirconium and titanium implants: Impact on image quality. Dentomaxillofacial Radiol. 2018;47(6).

40. Queiroz PM, Groppo FC, Oliveira ML, Haiter-Neto F, Freitas DQ. Evaluation of the efficacy of a metal artifact reduction algorithm in different cone beam computed tomography scanning parameters. Oral Surg Oral Med Oral Pathol Oral Radiol [Internet]. 2017 Jun;123(6):729–34. Available from: https://linkinghub.elsevier.com/retrieve/pii/S2212440317300949

41. Fontenele RC, Santaella GM, Freitas DQ. Does the metal artifact reduction algorithm activation mode influence the magnitude of artifacts in CBCT images ? 2020;23–30.

42. Nascimento EHL, Gaêta-Araujo H, Fontenele RC, Oliveira-Santos N, Oliveira-Santos C, Freitas DQ. Do the number of basis images and metal artifact reduction affect the production of artifacts near and far from zirconium dental implants in CBCT? Clin Oral Investig. 2021;25(9): 5281–91.

43. Sheikhi M, Behfarnia P, Mostajabi M, Nasri N. The efficacy of metal artifact reduction (MAR) algorithm in cone-beam computed tomography on the diagnostic accuracy of fenestration and dehiscence around dental implants. J Periodontol [Internet]. 2020 Feb 28;91(2):209–14. Available from: https://onlinelibrary.wiley.com/doi/10.1002/JPER.18-0433

44. Kamburoğlu K, Murat S, Kiliç C, Yüksel S, Avsever H, Farman A, et al. Accuracy of CBCT images in the assessment of buccal marginal alveolar peri-implant defects: Effect of field of view. Dentomaxillofacial Radiol [Internet]. 2014 May;43(4):20130332. Available from: http://www.birpublications.org/doi/10.1259/dmfr.20130332

45. De-Azevedo-Vaz SL, Peyneau PD, Ramirez-Sotelo LR, Vasconcelos K de F, Campos PSF, Haiter-Neto F. Efficacy of a cone beam computed tomography metal artifact reduction algorithm for the detection of peri-implant

fenestrations and dehiscences. Oral Surg Oral Med Oral Pathol Oral Radiol [Internet]. 2016 May;121(5):550–6. Available from: https://linkinghub.elsevier.com/retrieve/pii/S2212440316000158

46. Koç C, Kamburoğlu K, Sönmez G, Yılmaz F, Gülen O, Karahan S. Ability to detect endodontic complications using three different cone beam computed tomography units with and without artefact reduction modes: an ex vivo study. Int Endod J. 2019;52(5):725–36.

47. Cohen JF, Korevaar DA, Altman DG, Bruns DE, Gatsonis CA, Hooft L, et al. STARD 2015 guidelines for reporting diagnostic accuracy studies: Explanation and elaboration. BMJ Open. 2016;6(11):1–17.

48. R Foundation for Computing. R Core Team (2017). R: A language and environment for statistical computing R Foundation for Statistical. URL: https://www.r-project.org/ [Internet]. 2017. Available from: https://www.r-project.org

49. Sarao SK, Berlin-Broner Y, Levin L. Occurrence and Risk Factors of Dental Root Perforations: A Systematic Review, Vol. 71, International Dental Journal, Elsevier B.V.; 2021. p. 96–105.

50. Kim M-J, Lee S-S, Choi M, Yong HS, Lee C, Kim J-E, et al. Developing evidence-based clinical imaging guidelines of justification for radiographic examination after dental implant installation. BMC Med Imaging. 2020;20(1):1–9.

51. Vasconcelos T, Nascimento E, Bechara B, Freitas D, Noujeim M. Influence of Cone Beam Computed Tomography Settings on Implant Artifact Production: Zirconia and Titanium. Int J Oral Maxillofac Implants. 2019;34(5):1114–20.

52. Gaalaas L, Tyndall D, Mol A, Everett ET, Bangdiwala A. Ex vivo evaluation of new 2D and 3D dental radiographic technology for detecting caries. Dentomaxillofacial Radiol [Internet]. 2016 Mar;45(3):20150281. Available from: http://www.birpublications.org/doi/10.1259/dmfr.20150281

53. Baltacıoğlu İH, Eren H, Yavuz Y, Kamburoğlu K. Diagnostic accuracy of different display types in detection of recurrent caries under restorations by using CBCT. Dentomaxillofacial Radiol [Internet]. 2016 Jul;45(6):20160099. Available from: http://www.birpublications.org/doi/10.1259/dmfr.20160099

54. Majhi R, Majhi RK, Garhnayak L, Patro TK, Dhal A, Kumar S, et al. Comparative evaluation of surface-modified zirconia for the growth of bone cells and early osseointegration. J Prosthet Dent [Internet]. 2021 Jul;126(1):92.e1-92.e8. Available from: https://linkinghub.elsevier.com/retrieve/pii/S0022391321002249

55. Gaêta-Araujo H, Nascimento EHL, Fontenele RC, Mancini AXM, Freitas DQ, Oliveira-Santos C. Magnitude of beam-hardening artifacts produced by gutta-percha and metal posts on cone beam computed tomography with varying tube current. Imaging Sci Dent. 2020;50(1):1–7.

56. Senthilkumar V, Subbarao C. Management of root perforation: A review. J Adv Pharm Educ Res. 2017; 7(2):54–7.

57. Shahmirzadi S, Sharaf RA, Saadat S, Moore WS, Geha H, Tamimi D, et al. Assessment of the efficiency of a pre- versus post-acquisition metal artifact reduction algorithm in the presence of 3 different dental implant materials using multiple CBCT settings: An in vitro study. Imaging Sci Dent. 2021;51:1–7.

58. Orhan AI, Tufenkci P, ONCU A, Sevgi S, Celikten B, Orhan K. CBCT Visualization of Furcation Perforation Repair Materials Using Different Voxel Sizes, Clin Exp Heal Sci. 2021;(8).

59. Koç C, Sönmez G, Yılmaz F, Karahan S, Kamburoğlu K. Comparison of the accuracy of periapical radiography with CBCT taken at three different voxel sizes in detecting simulated endodontic complications: An ex vivo study. Dentomaxillofacial Radiol. 2018;47(4):1–9.